A biobased epoxy vitrimer/cellulose composite for 3D printing by Liquid Deposition Modelling

(Article begins on next page)

01 September 2024

A biobased epoxy vitrimer/cellulose composite for 3D printing by Liquid Deposition Modelling

Jerome M. Capannelli [a,b], Sara Dalle Vacche [a], Alessandra Vitale [a,c], Khaoula Bouzidi [b], Davide Beneventi [b,**], Roberta Bongiovanni [a,c,*]

[a] *Department of Applied Science and Technology, Politecnico di Torino, Corso Duca Degli Abruzzi 21, 10129, Torino, Italy*
[b] *Univ. Grenoble Alpes, CNRS, Grenoble INP (Institute of Engineering Univ. Grenoble Alpes), LGP2, 38000, Grenoble, France*
[c] *INSTM-Politecnico di Torino Research Unit, 50121, Firenze, Italy*

ARTICLE INFO

ABSTRACT

Conventional epoxy polymers are obtained from oil-based resources and their structure is formed by permanent covalent crosslinks. Therefore, this class of materials is now considered non environmentally friendly as they are neither renewable nor reprocessable and recyclable. In this study, we prepared a vitrimeric material based on an epoxy-functionalised cardanol cured with a biobased polycarboxylic acid. In the presence of a zinc-containing catalyst, a soft polyester with a $T_g = -13$ °C was obtained; its reprocessability by a chemical method was demonstrated to be feasible without any relevant change in properties once a second curing cycle was completed. The vitrimeric polyester was then used in combination with cellulose powder for the preparation of a sustainable and biobased composite. The matrix/filler mass fraction was tailored to obtain a composite paste with suitable rheological properties for 3D printing via Liquid Deposition Modelling (LDM). Preliminary printing tests were successful, and the vitrimeric printed parts were then thermally cured retaining the shape. The suitability of the vitrimeric composite for additive manufacturing was thus confirmed: the new material can provide a solution to 3D printing of recyclable thermosetting biobased polymers.

1. Introduction

The demand for more sustainable polymeric materials, whether biobased and/or recyclable, has been increasing for decades. In this scope, substitution of thermosets, which are permanently crosslinked polymers and cannot be reprocessed nor reshaped, is required. To this aim, new types of polymeric networks called Covalent Adaptable Networks (CANs) or Dynamic Covalent Networks (DCNs) have been developed (N. [1,2]; Z. P. Zhang, Rong, et [3,4]: CANs can be defined as polymeric materials that exhibit covalent crosslinks that are reversible under a specific stimulus, such as heat (J. [1], thus retaining the performances of thermosets and combining them with the ability of thermoplastics of being malleable and reprocessable. In detail, CANs are classified into two groups, associative and dissociative CANs [5]. For dissociative CANs, recyclability is assured by dissociative exchange mechanisms, such as Diels-Alder reactions: dissociation causing a drop in crosslinking density brings fluidity and thus reprocessability, but it is

detrimental to material performance, e.g., solvent resistance is usually lost. On the contrary, associative CANs are based on dynamic exchange mechanisms without any change in crosslinking density: different bonds are broken and formed at the same time, which allows maintaining the material performance unchanged, e.g., solvent resistance. The breakthrough regarding the class of associative CANs was the synthesis of vitrimers by Leibler's group in 2011 [6]. The word "vitrimer" was suggested by observing that the polymer showed a viscosity change upon heating as vitreous silica materials. Then a characteristic temperature was defined, called topology freezing transition temperature T_v, above which the material flows and its viscosity changes following an Arrhenius trend. For the development of vitrimers, many exchangeable reactions have been investigated, such as disulfide [7,8]; Luzuriaga et al., 2016; [9], imine bonds [10–12], vinylogous urethane [13], boronate ester [14,15] or hindered urea [16]; D. [17], in addition to transesterification reactions [18–20], which are still the most exploited since the first work on epoxy vitrimers [6]. In these systems, the reaction

---

can involve either the ester groups formed during the hardening reaction of acids or anhydrides and epoxides or those initially present in the epoxy/hardener backbones. The polymer recycling based on transesterification can be a mechanical or a chemical process. In the first case, the vitrimer is grinded and then reshaped with a compression moulding machine at high temperature and high pressure, such as 180 °C and 40 bar [19]. This approach is the most straightforward, but costly; moreover, if a composite must be treated, it implies damage to the reinforcement phase. Alternatively, the vitrimer can be chemically recycled by dissolution by an alcohol such as ethylene glycol, or water: the solvent swells the network and takes part in the transesterification reaction cleaving the chains. After dissolution, by heating the system at high temperature (around 180 °C), the solvent evaporates and the crosslinked structure is restored [19,21].

Therefore, epoxy vitrimers are not only reprocessable as thermoset, but they can be processed and reprocessed as thermoplastics through conventional shaping processes, i.e., extrusion and injection moulding. As the development of epoxy vitrimers targets materials having large industrial interest and commercial relevance, their implementation is likely to be simple and with a high impact making a great change in industry. Moreover, in the case of composites, the thermally activated bond exchange via transesterification, which allows the polymeric matrix to flow at high temperature, gives the option of recycling the material as it is or isolating the matrix and reclaiming the filler [19,22].

Further interest for these innovative epoxy networks is their application in the field of additive manufacturing (AM) [23]. At present, common AM technologies for epoxides are stereolithography and related techniques, and ink writing, employing photosensitive formulations as common practice. Thermoset epoxides are also demonstrated suitable for jetting techniques, and few examples concerning extrusion techniques are found in literature, even applied to epoxy-based vitrimers using adapted Fused Deposition Modelling [20,23]. However, to the best of our knowledge, no examples of processing epoxy vitrimers by cold Liquid Deposition Modelling (LDM), are present in the literature. LDM is an extrusion-based 3D printing technique [24] and is currently applied for the processing of ceramics, wood and food pastes. However, it is attractive compared to the other AM technologies cited above, as it has lower costs, uses a simple set up working at room temperature, and has good potential for producing large size pieces.

Besides developing applications by 3D printing, a further challenge in the field of vitrimers is the use of sustainable raw materials. Different groups reported the synthesis of partially or fully biobased vitrimers [7] starting from vegetable oils, lignin derivative such as vanillin [7] or furan-based precursors (Dhers, Vantomme, et Avérous 2019). Few interesting reviews were recently published on the topic [25–27]. In the case of epoxy vitrimers based on transesterification reactions, they can be synthesized using biobased epoxy resins and biobased hardeners, where the ester groups are either present in the backbone of the precursors or are formed during their hardening, i.e., employing acids or anhydrides as co-reactants [25]; Y [28,29].

Considering the perspective of applying epoxides in AM and taking into account the demand of sustainability, in this work we prepared an environmentally benign epoxy vitrimer composite suitable for extrusion 3D printing: to this aim we employed precursors with a high biobased content and cellulosic powder both as reinforcement and rheology modifier. First, the biobased epoxy vitrimer matrix was synthesized, and its chemical recycling was investigated; then, by adding cellulose powder, the rheological behaviour of the composite was tuned and printability by LDM process was assessed fabricating a simple demonstrator.

2. Materials and methods

2.1. Materials

The synthesized epoxy vitrimer was based on epoxidized cardanol NC-514S, supplied by Cardolite®, with an epoxide equivalent weight of

438 g/eq and average functionality f = 1.1 [30]. A mixture of fatty dicarboxylic and tricarboxylic acid, Pripol 1040, with an acid equivalent weight of 296 g/eq and 100% biobased content, was used as crosslinker and kindly provided by Croda Ltd. The chemical structure of the epoxy precursor and of the dimer/trimer acid is reported in Fig. 1. The catalyst used was zinc acetate $Zn(Ac)_2$ and was purchased from Carl Roth.

For the composite, a commercial cellulose powder, Technocel® FM8, was supplied by CFF GmbH & Co. KG and used as a filler without any pretreatment. According to the datasheet, particle diameter is reported to be between 6 and 12 μm, as also confirmed in a previous work [31].

Acetone (≥99.0% pure) was supplied by Acros Organics, ethylene glycol was purchased from Carl Roth. All the products were used as received.

2.2. Preparation and curing of the vitrimer

The vitrimer was prepared in a single step: the epoxidized cardanol NC-514S, the dimer/trimer acid and the catalyst $Zn(Ac)_2$, either with or without cellulose powder, were mixed in a planetary mixer (KitchenAid 5KSM3311X) at room temperature at 120 rpm for 5 min and then at 200 rpm for additional 5 min. Before any curing, the samples were stored in the fridge at 4–5 °C to prevent any crosslinking during storage. The systems were thermally cured in oven at 200 °C for 6 h after pouring the mixture in a PTFE mould.

In detail, NC-514S and acid were mixed maintaining an equimolar ratio epoxide/COOH groups. $Zn(Ac)_2$ concentration was 10 mol% with respect to acid groups. In a typical formulation of 100 g, 58.21 g of NC-514S, 39.35 g of Pripol 1040 and 2.44 g of $Zn(Ac)_2$ were mixed. Cellulose powder weight fraction was in the range of 30–42 wt% with respect to the total mass of the composite.

2.3. 3D printing

The 3D printing was performed by LDM using a commercial benchtop 3D printer (Artillery Sidewinder X1) after proper customization. The printer, originally designed to print fused filaments, was upgraded by adding a screw extruder (WASP claystruder) with a nozzle diameter of 0.7 mm, fed by a syringe under pressure at 3 bars to ensure proper feeding. The software Simplify3D® was used as slicer.

After the flow calibration of the screw extruder, 3D printing was carried out with a fixed layer height of 0.4 mm, a printing speed of 500 mm/min and infill of 60% with 45/-45° angles. After printing, the objects were thermally cured following the same thermal process applied for the neat vitrimer, i.e., heating at 200 °C for 6 h.

2.4. Vitrimer chemical recycling

The recycling process was performed adapting the procedure described in Ref. [20]. The cured samples were cut in pieces of around 10 x 10 × 5 mm^3 and immersed in a bath of ethylene glycol that was heated at 180 °C under reflux for 6 h. After dissolution, the obtained solution was distilled for 6 h at 180 °C under vacuum to recycle both the vitrimer and the ethylene glycol.

2.5. Characterization

Fourier Transform Infrared (FT-IR) analysis was performed in attenuated total reflection (ATR) mode (PerkinElmer, Spectrum65) using the universal ATR sampling accessory equipped with a diamond crystal. The spectra were acquired in the 600–4000 cm^{-1} range, with 32 scans per spectrum and a resolution of 4 cm^{-1}.

Thermogravimetric analysis (TGA) was performed using a TGA/DSC 3+ StarSystem from Mettler Toledo. Measurements were performed from 25 °C to 800 °C with a heating rate of 10 °C/min, under N_2 flux, preventing any thermo-oxidative process, and from 800 °C to 900 °C with a heating rate of 10 °C/min, under air flux. First order derivative of
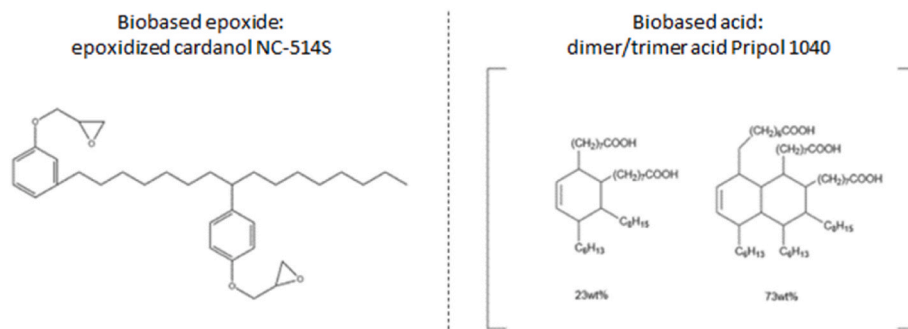
Fig. 1. Chemical structures of the biobased epoxide NC-514S and biobased hardener Pripol 1040.

the weight profile was calculated by Origin (OriginLab) software to better observe the main degradation temperatures of the produced samples.

Differential scanning calorimetry (DSC) was performed using a DSC Q100 from TA Instrument. The measurements were conducted making a first heating at 20 °C/min from 25 °C to 100 °C to remove any thermal history in the sample, followed by two cycles from −100 °C to 280 °C at a heating rate of 10 °C/min under N$_2$ flux. Glass transition temperature was taken as the inflection point in the second cycle.

Insoluble fraction and solubility tests were performed in acetone. Samples of around 0.5–1 g were wrapped in a metallic net with a mesh size of 100 μm and soaked in acetone for 24 h, then they were left drying for 48 h and the mass loss of the samples was calculated.

Rheological analyses were performed using an Anton Paar rotational rheometer MCR302 equipped with parallel plates ($\varphi = 25$ mm, gap = 1 mm). Apparent viscosity was measured in the shear rate range of 0.1 s^{-1} to 100 s^{-1}. Viscoelastic properties were measured on the same instrument with the Amplitude Sweep Test at a frequency of 1 Hz and strain ranging from 0.001% to 100%. The evolution of both the storage modulus (G′) and the loss modulus (G″) as a function of stress was analysed.

Relaxation tests were performed on the same rotational rheometer using cured samples with $\varphi = 40$ mm and 1 mm thick gap. The sample was placed between parallel plates and contact was ensured by applying a 10 N normal force. After the set temperature was reached, the sample was equilibrated for 20 min before starting the measurement. Relaxation measurements were performed by applying a shear strain of 2% in the linear viscoelastic region of the material.

3. Results and discussions

3.1. Preparation and characterization of biobased vitrimer

The biobased epoxy vitrimer was synthesized using a commercial biobased resin (NC–514S), obtained by epoxidation of cardanol, a phenolic lipid found in the cashew nutshell liquid (CNSL), and a mixture of dicarboxylic and tricarboxylic fatty acids having 100% renewable carbon content (Pripol 1040) as a hardener. Their chemical structures are shown in Fig. 1.

The curing of the resin, leading to the biobased vitrimer, was made by heating at 200 °C for 6 h, in the presence of Zn(Ac)$_2$. At the end of the treatment, a solid was obtained with a highly insoluble content (90.2%, in acetone), while the starting raw materials were fully soluble in acetone. As described by Demongeot [32] and sketched in Fig. 2, the

crosslinking process is due to the reaction of the oxirane rings of the multifunctional epoxide NC-514S with the carboxylic groups of the hardener Pripol 1040, forming ester bonds.

The completion of the esterification reaction was controlled by ATR-FT-IR spectroscopy. Fig. 3 reports the spectra of the epoxy/acid system before and after heating (i.e., curing): we can easily observe the complete disappearance of the band related to epoxide at 910-915 cm^{-1}, the shift of the band attributed to the carboxylic acids from 1715 cm^{-1} to a higher value, around 1740 cm^{-1}, related to ester groups, and additionally the appearance of a broad peak at around 3400 cm^{-1} due to hydroxyl groups. All these results assess the ring opening of the oxirane groups and their esterification, clearly confirming the successful crosslinking of the epoxy resin.

The obtained cured solid polyester (i.e., vitrimer) was characterized by thermal analyses, i.e., DSC and TGA. In Fig. 4, the DSC thermograms of the material before and after curing are compared. The uncured epoxy/acid system shows a glass transition temperature (T_g) at around −50 °C, which is comparable to the T_g of pure epoxy resin, known to be around −48 °C [33]. After the heating cycle, the crosslinked polyester has a higher T_g at −13 °C, as expected: the network is however in its rubbery state at room temperature and at the common service
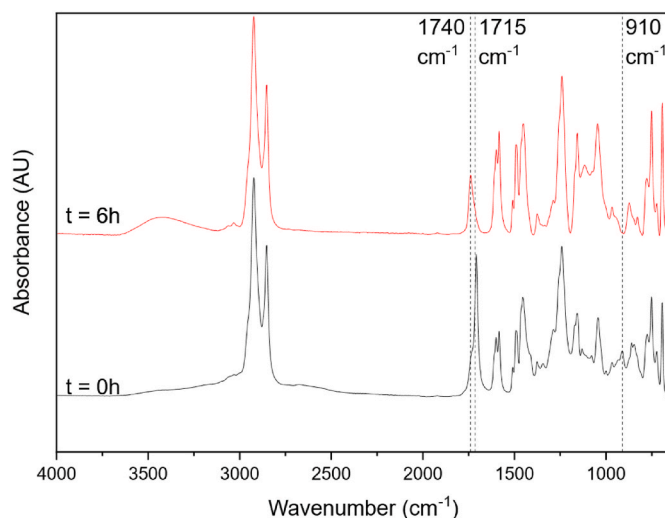

Fig. 3. ATR-FT-IR spectra of the epoxy/acid system before (t = 0 h) and after (t = 6 h) curing.
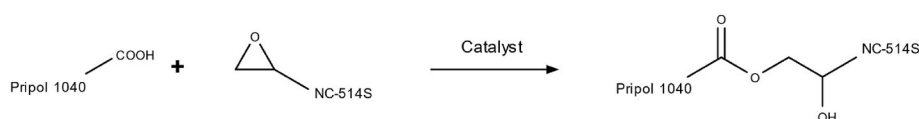

Fig. 2. Esterification reaction between the epoxy resin and the acid, in the presence of zinc catalyst.
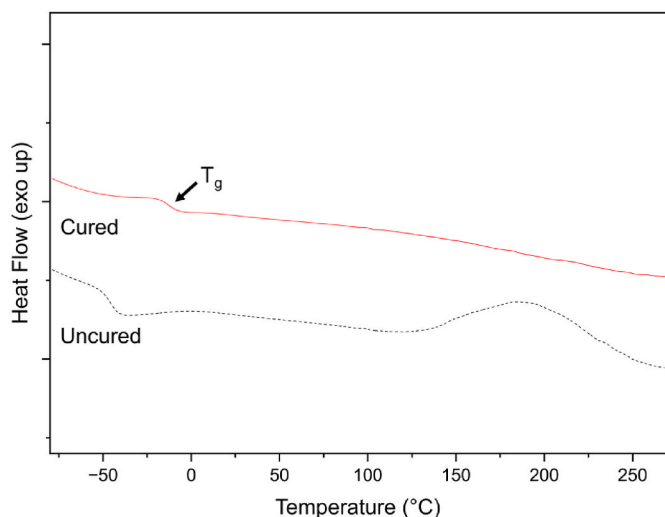
Fig. 4. DSC thermograms of the epoxy/acid system before and after curing.

Material	T_5 (°C)	T_{50} (°C)	$m_{800°C}$ (%) Under N_2	$m_{900°C}$ (%) Under air
Cured vitrimer	319	443	6	3
NC-514S	296	408	3	0

temperatures. In the DSC curve of the uncured polymer (Fig. 4) above 150 °C, an exothermic broad peak is present, which disappears upon heating: this signal is related to the enthalpy of the esterification reaction and its disappearance confirms the completion of the crosslinking. The heat of the esterification reaction obtained by the signal integration was used to evaluate the enthalpy value of the epoxy ring opening reaction of the system under investigation: the ΔH value is 56 kJ mol^{-1}, which is rather close to the mean value of the molar reaction enthalpy reported in the literature for commercial epoxies, i.e., 65 ± 3 kJ mol^{-1} [34].

Fig. 5 shows the TGA curve of the cured vitrimer and of the pure epoxy resin (NC–514S). As reported in Table 1, upon heating under inert atmosphere, the cured vitrimer shows the onset of the degradation (T_5, i. e., the temperature corresponding to a mass loss of 5%) at 319 °C, while the main degradation happens at a higher temperature, and T_{50} (i.e., the temperature corresponding to a mass loss of 50%) is at 443 °C. Compared to the pure liquid resin NC-514S, the degradation of the crosslinked polymer is shifted to higher temperature as expected.

Additionally, data reported in Table 1 show that the cured polyester has a higher residual mass at 800 °C, ca. 6%, than the pure resin, further suggesting that the crosslinking between the epoxy and the acid took place. Heating under air up to 900 °C the organic matter is thermally
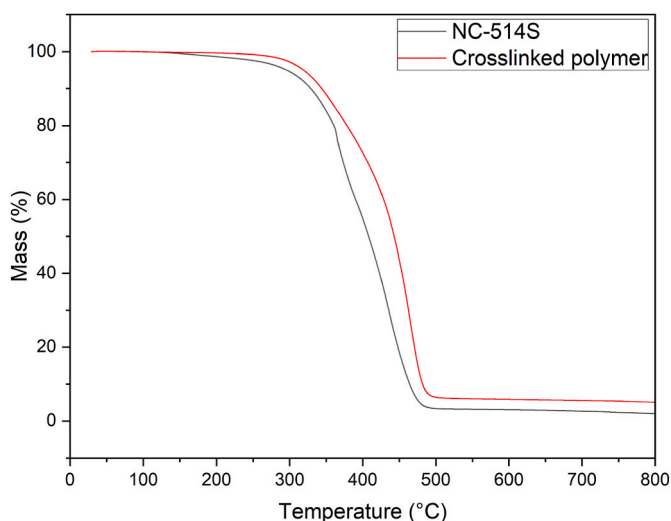
oxidized, for the pure resin the residue is zeroed, while the value for the crosslinked polymer decreases to ca. 3%, slightly higher than the initial mass of catalyst.

It was demonstrated in many works [2] that covalent adaptable networks show temperature-frequency-dependency of the storage (G′) and loss (G″) moduli, while thermosets formed by permanent covalent bonds display a temperature-frequency-independent storage (G′) modulus. Therefore, we studied the viscoelasticity of our network by stress relaxation experiments at different temperatures, applying a small deformation (2%) and adopting the Maxwell model to estimate the relaxation time τ (Eq. (1)):

$$\frac{G'}{G_0} = e^{-\frac{t}{\tau}} \qquad \text{Eq. 1}$$

where G_0 is the initial value of the storage modulus, t is the time, and the relaxation time τ corresponds to the time for which G'/G_0 = 1/e = 0.37.

In Fig. 6A, the G' values for the cured vitrimer sample at different temperatures, normalized over G_0, are reported as a function of time: the elastic response of the cured polyester is clearly changing depending on time and temperature, thus exhibiting the behaviour of an adaptable covalent network. As expected, we observed faster stress relaxation at higher temperatures (Fig. 6A): the relaxation time of our vitrimer ranges from ≈1200 s at 200 °C up to ≈ 10000 s at 160 °C. These relaxation times are longer than those for epoxy vitrimers based on the most common epoxide, bisphenol-A diglycidyl ether (DGEBA), cured with the same fatty acids in the same equimolar ratio as in the present work: for the DGEBA based network τ ≈ 300 s at 200 °C and τ ≈ 1500 s at 160 °C [21]. This is a striking difference: as the molecular mechanism of the underlying chemical exchange was the same, having used the same catalyst at a slightly higher concentration, one could even expect a faster reaction than for the DGEBA vitrimer. It is evident that other parameters can possibly govern the dynamic properties of epoxy vitrimers and in recent papers they were identified as chain mobility, synergies of different dynamic bonds and density of exchangeable bonds [[35–37]]. In our case, looking at the structures of the polyesters under comparison, presence of different dynamic bonds and neighbouring group participating and/or influencing the exchange reaction of DGEDA polyester cannot be found. Meanwhile chain mobilities are different: as the aromatic DGEBA network has a higher T_g (i.e., 33 °C versus −13 °C) than the novel biobased polyester, the latter should show an easier molecular diffusion, favouring transesterification, which is not. The density of the exchangeable bonds is another difference between the networks: the investigated biobased vitrimer has a much lower crosslinking density ν_e than DGEBA [21] due to the difference in functionality (Cardolite has an average functionality f = 1.1, with epoxy equivalent weight = 438 g/eq, while DGEBA has f = 2, with epoxy equivalent weight = 172 g/eq) being the epoxy-acid conversion quantitative for both systems (the calculation of ν_e for the investigated vitrimer network can be found in the Supporting Information). The effect of the ν_e value on relaxation time is discussed in detail for model systems of epoxides cured with Pripol by Chen [38] and it is demonstrated that the typical stress relaxation behaviour of epoxy vitrimers is accelerated increasing crosslinking density ν_e. Thus, the lower concentration of ester bonds of the fully biobased vitrimer prepared from Cardolite epoxide and a biobased acid causes longer relaxation times with respect to the DGEBA polyester formed with the same acid. Overall, the choice of a proper f is likely to be
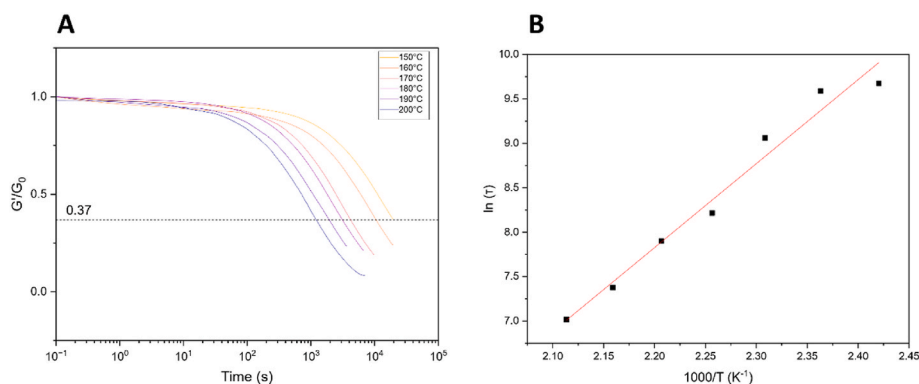

Fig. 5. TGA thermograms of the cured polyester network and of the pure epoxy resin.

Fig. 6. Viscoelasticity study of the cured vitrimer. A) Normalized stress relaxation curves at several temperatures. B) Plot of ln (τ) versus 1000/T.

crucial for designing a new vitrimer.

As in vitrimers bonds are only broken if new ones are already formed as a single thermally activated process, the relaxation time of the material changes with the temperature according to the Arrhenius law [39], as in Eq. (2):

$$\tau = \frac{1}{k} e^{\frac{E_a}{RT}} \qquad \text{Eq. 2}$$

where E_a is the activation energy of the exchange reaction, T is the temperature, R is the universal gas constant, and k is the pre-exponential factor. The relaxation time at different temperature as obtained from the G'/G$_0$ curves are plotted in Fig. 6B: the slope of the fitting curve corresponds to the coefficient E_a/R and thus E_a (kJ mol^{-1}) of the thermal process can be estimated. The E_a value has practical importance, as the higher it is the more rapid the decrease of viscosity and the faster the stress relaxation with rising temperatures: this means dimensional stability at the service temperature of the material and a faster processing on demand. In our case the activation energy for the bonds exchange is found $E_a \approx 85$ kJ mol^{-1} and is in agreement with the literature data for epoxy networks (J [1,6,38,40]. This means that the material under investigation can compete with traditional epoxy vitrimers.

From the viscoelasticity studies, the topology freezing temperature, T_v, of the polymer, was also estimated: it is defined as the temperature of transition of a material from a viscoelastic solid to a viscoelastic liquid. As this transition is considered to happen for a viscosity η of 10^{12} Pa s, first the corresponding relaxation time τ* can be calculated from the Maxwell model by Eq. (3):

$$\eta = G\tau* \qquad \text{Eq. 3}$$

obtaining G from the value of the storage modulus E' at the rubbery plateau according to Eq. (4):

$$G = \frac{E'}{2(1+\nu)} \qquad \text{Eq. 4}$$

where ν is the Poisson's ratio of the material, which can be assumed = 0.5 for rubbery materials.

The value of E' was obtained by dynamic mechanical analyses (DMA), which are reported in Fig. S1 of the Supporting Information. Once the relaxation time τ* was estimated by using Eq. (3), through the relationship ln(τ) versus 1000/T (see Fig. 6B), the value of T_v for the vitrimer network was found 71 °C (see the Supporting Information for the calculations).

3.2. Vitrimer chemical recycling

As already mentioned previously, the main interesting feature of CANs is their ability to be recycled/reprocessed. In this work, we performed the chemical recycling of the biobased epoxy vitrimer leveraging

the transesterification reaction with ethylene glycol (EG). As depicted in Fig. 7, after dissolution of the cured material in EG, the solvent was partially evaporated at high temperature to obtain a resin with the desired viscosity. Then, by further heating, the remaining solvent was distilled, and the crosslinked network was rebuilt with the aid of the Zn catalyst present in the vitrimer.

The macroscopic phase change of the material during the production/recycling cycle is shown in Fig. 8. The initial liquid resin formulation is first cured and transformed into a vitrimer, the vitrimer is recycled as a viscous resin (which is soluble in acetone), the resin can be cured again with the same curing conditions obtaining a solid, whose gel fraction was determined to be around 86%, which is only slightly lower than the one observed for the initial vitrimer (90%). It is evident that the reprocessed sample is darker than the original network: this is likely to be due to thermal oxidation as explained in the literature [20].

Besides the visual observations, the recycled vitrimer was subjected to spectroscopic and thermal testing. The ATR-FT-IR spectrum of the original resin and of the resin after transesterification (i.e., EG-dissolved vitrimer) are compared in Fig. 9A: as expected, the recycled product does not contain epoxy groups (no peak appears at 910-915 cm^{-1}), while it is still exhibiting the ester related peak at 1740 cm^{-1}. Therefore, this suggests that de-crosslinking is not occurring. However, an increase of the absorbance of the band at around 3400 cm^{-1} related to the hydroxyl groups can be noted: this could indicate the presence of remaining ethylene glycol.

The ATR-FT-IR spectra of the vitrimer freshly cured and the one cured after recycling are reported in Fig. 9B: interestingly, one can notice but negligible differences between the two products, thus the chemical integrity of the material upon recycling was confirmed.

Concerning the thermal behaviour of the material after recycling, no major difference can be observed both by DSC and TGA. When comparing the DSC spectra of the pristine sample and that of the recycled one (Fig. 10) same glass transition temperatures are measured ($T_g \approx -13$ °C), and no exothermic peak is found in both curves (i.e., curing is complete). Similar conclusions come from TGA measurements: the degradation profile for both the pristine network and the recycled vitrimer are similar.

The viscoelastic behaviour of the network after recycling was also investigated. As described above, the relaxation time τ and the activation energy E_a of the recycled material were determined from the relaxation curves given in Fig. 11A and from the relationship between τ and temperature (τ values at different temperatures are plotted in Fig. 11B). Data of the neat vitrimer and of the recycled one are compared in Table 2. As one can observe, relaxation time is greater for the recycled vitrimer than for the initial vitrimer. These changes might be due to the loss of catalyst during the recycling process or to side-reactions, such as etherification, that are reducing the efficiency of the transesterification. On the other hand, the activation energy was determined to be 110 kJ mol^{-1}, which is consistent with literature (J [1]. for transesterification
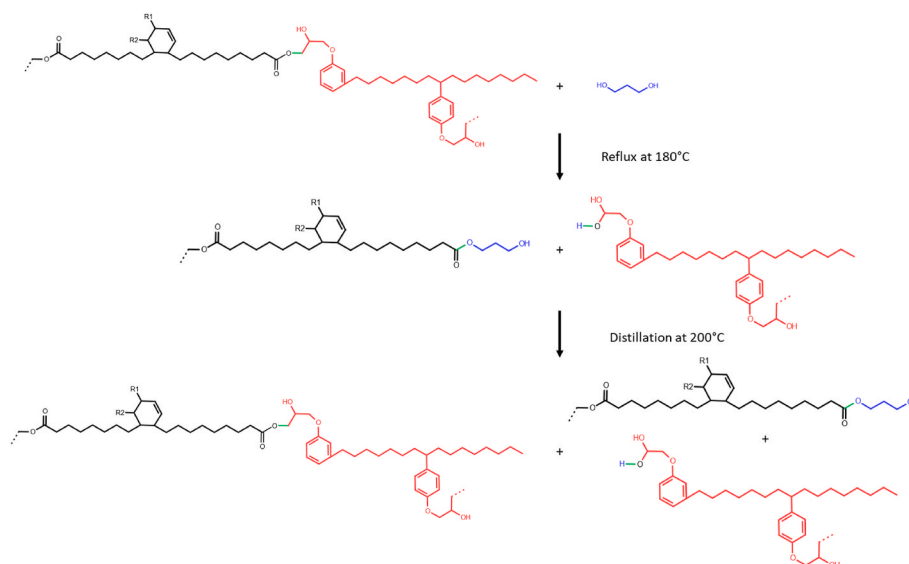
Fig. 7. Chemical recycling route, adapted from Ref. [21].

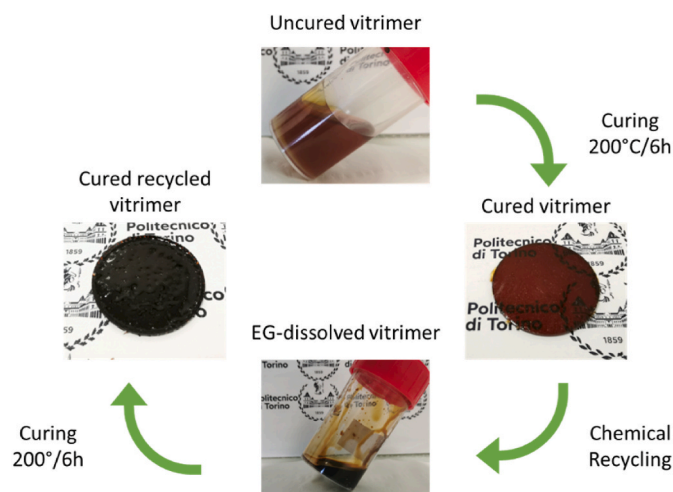## 3.3. Vitrimer printing by LDM: addition of cellulosic powder

Fig. 8. Production and recycling cycle of the biobased epoxy vitrimer.

mechanisms. However, it is greater than the one of freshly cured vitrimer ($\approx$85 kJ mol^{-1}): this could confirm the occurrence of competitive reactions, such as etherification and thermo-oxidation.

LDM is an AM method suitable for thermoplastics but adopted for thermoset resins. For this class of materials after the two main printing steps, extrusion and deposition, a curing step must follow. Each printing step requires different viscoelastic features. For being extruded the resin should exhibit shear-thinning behaviour, while for the deposition phase, when the uncured resin must hold the shape, yield stress and stiffness must be maximized [31,41]. Guidelines for successful LDM printing based on the results obtained in a previous work [42] are: strong shear thinning behaviour, apparent viscosity η from approx. 10^4 Pa s at 0.1 s^{-1} to 10 Pa s at 10^2 s^{-1}; yield stress τ_y in the range 10^2–10^3 Pa; stiffness G' between 10^4 and 10^5 Pa. Apparent viscosity measurement performed on the vitrimer precursors is shown in Fig. 12A (black curve): it indicates that the epoxy resin and the acid hardener mixture does not satisfy any of the above criteria.

Therefore, we decided to add a rheology modifier: a cellulose powder was preferred being biobased, widely available and cheap. To minimize the risk of clogging of the extruder, the cellulosic filler had particle size below 12 μm as it should not exceed 1/100th to 10/100th of the nozzle diameter of 0.7 mm [42].

Viscosity curves were recorded for different contents of cellulose powder, from 30 to 42 wt% (Fig. 12A). The apparent viscosity of the mixtures with a different content of cellulose varied from 2000 Pa s to 40000 Pa s at 0.1 s^{-1} and it was above 100 Pa s at 10^2 s^{-1} for any composition. The flow curves were fitted according to the Ostwald–De
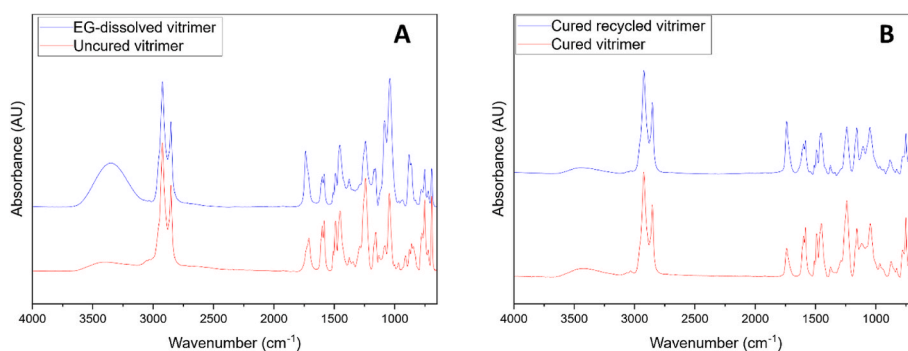

Fig. 9. ATR-FT-IR spectroscopy analysis of the vitrimer, before and after chemical recycling. A) Spectra of uncured vitrimer and of EG-dissolved vitrimer. B) Spectra of cured vitrimer and cured recycled vitrimer.
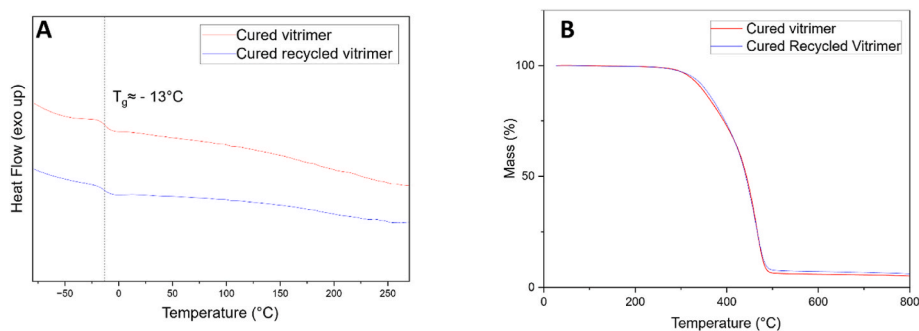
Fig. 10. Thermal analysis of the vitrimer, before and after chemical recycling. A) DSC thermograms of cured vitrimer and of cured recycled vitrimer. B) TGA of cured vitrimer and of cured recycled vitrimer.
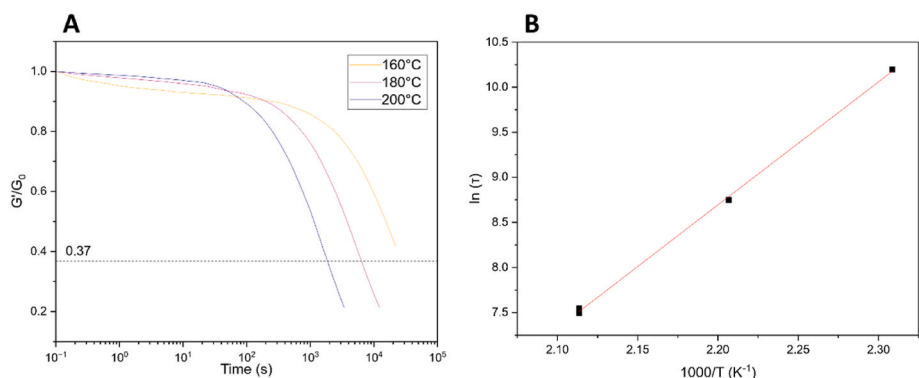

Fig. 11. Viscoelasticity study of the recycled vitrimer. A) Normalized stress relaxation curves at three different temperatures for the cured recycled vitrimer. B) Plot of ln (τ) versus 1000/T.

Table 2
Relaxation time of cured vitrimer and cured recycled vitrimer at different temperature values.

Temperature (°C)	Relaxation time (s)	
	Cured vitrimer	Cured recycled vitrimer
200	≈1200	≈1800
180	≈3000	≈6300
160	≈10000	≈26800[a]

[a] The relaxation time at 160°C for the cured recycled vitrimer is a projected value.

Waele power law (Eq. (5)):

$$\eta = K\dot{\gamma}^{n-1} \qquad \text{Eq. 5}$$

where K is the consistency index and n is the thinning exponent. K is related to the viscosity at low shear rate, at rest, whereas n defines the rheologic behaviour of the material and when $n = 0$ the ideal shear-thinning behaviour is observed. In Fig. 12B, K and n are plotted as a function of filler concentration. As expected, the higher the cellulose powder content, the higher the K value; $n = 0.96$ for the pure resin, then it diminishes and reaches a value of 0.1–0.3 when the cellulose content is 37–42 wt%.

Stiffness G$'$ and yield stress τ_y were measured by the Amplitude Sweeps Test: the obtained curves are plotted in Fig. 13A. G' value was taken as the value of the storage modulus in the Linear Viscoelastic

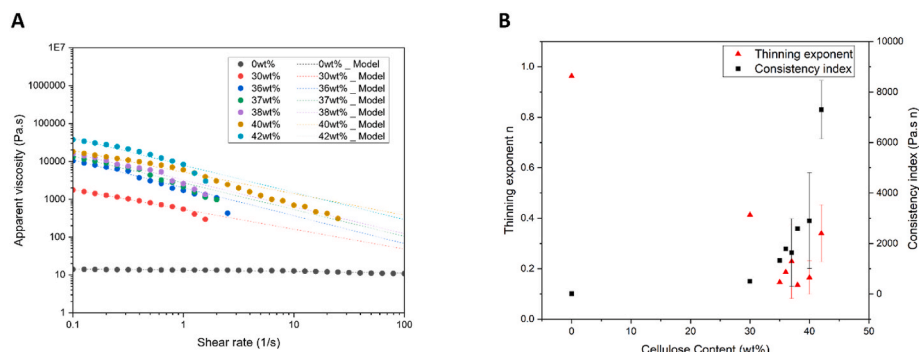**Fig. 12.** Rheologic characterization of the vitrimer filled with different contents of cellulose powder. A) Apparent viscosity of the vitrimer and of a selection of composites. For the composites measurements stopped due to measuring issues at high shear rate, such as rip-off of samples. The experimental curves are fitted with the Ostwald–De Waele power law (Eq. (5)). B) Consistency index and thinning exponent for the composites.
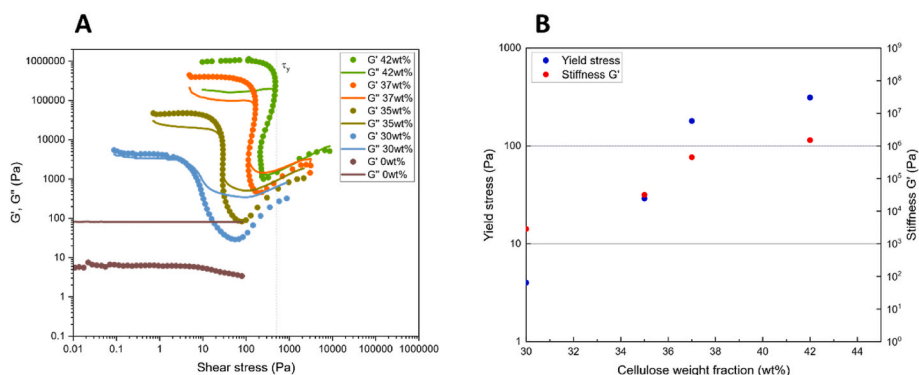
Fig. 13. Amplitude Sweep Test results of the epoxy vitrimer filled with different contents of cellulose powder. A) Storage and loss modulus obtained in Amplitude Sweep Test at 1 Hz. B) Stiffness G′ and yield stress τ_y for composites with cellulose content $\geq$30 wt%.

Region (LVER). τ_y, i.e., the minimum stress required for the resin to start flowing, was evaluated according to the Herschel-Bulkley model for a non-Newtonian fluid exhibiting a yield stress τ_0 (Eq. (6)):

$$\tau = \tau_0 + K\dot{\gamma}^n \qquad \text{Eq. 6}$$

where K is the consistency index and n is the dimensionless flow index. The obtained values for the stiffness G′ and the yield stress τ_y are reported in Fig. 13BFig. 1: both are increasing as a function of the filler content, as expected.

With a content of at least 37 wt% of cellulose filler, both stiffness (G′ = 3×10^5 Pa) and yield stress (τ_y = 150 Pa) are satisfying the criteria of printability (i.e., τ_y in the range 10^2–10^3 Pa and G′ between 10^4 and 10^5 Pa). This composition was therefore chosen for curing and further characterization in view of printing trials.

The curing of the composite was performed in the same conditions of the neat resin (200 °C, 6 h), and by ATR-FT-IR (Fig. 14) the successful crosslinking of the vitrimer in the presence of filler was demonstrated. As for the pure epoxy resin and acid hardener, also in the presence of cellulose filler, the disappearance of the epoxide band at 910–915 cm^{-1} and the shift of the carbonyl band from 1715 cm^{-1} to a higher wavenumber, 1740 cm^{-1}, assessing the transformation of the carboxylic group into the ester group, are observed with curing. As for the initial resin, a broad peak at around 3400 cm^{-1}, which is related to the hydroxyl groups, can also be detected. This result is particularly interesting as the hydroxyls will be also used for the dynamic transesterification reaction. In the FT-IR spectra of Fig. 14, one can clearly identify bands

due to cellulose in the region around 1100 cm^{-1}.

Successful crosslinking was also confirmed by the high value of the insoluble fraction (94%). Main thermal properties of the cured composite are listed in Table 3, and compared to those of the cured vitrimer. The T_g of the composite measured by DSC was found close to the one of the vitrimer, with a value around −15 °C. In the TGA curve of the composite, in addition to the vitrimer degradation, an early degradation at 300 °C due to the cellulose powder can be detected. Therefore, the degradation characteristic temperatures of the composite are lower than those of the neat vitrimer (Table 3). Residual masses at 800 °C for the composite are higher due to the presence of the filler.

Preliminary tests on chemical recycling were performed also for the composite sample, applying the same procedure as for the neat vitrimer (reaction described in Fig. 7). The ATR-FT-IR spectrum of the recycled composite had no noticeable difference with respect to the pristine composite (Figure in the Supporting Information). However, a change in T_g was measured with a shift from −15 °C to −21 °C after recycling. This suggests that with the recycling process a slightly different network can be obtained. Additionally, although the thermal degradation profiles were almost the same, small differences in the characteristic degradation temperatures are present, as reported in Table 3. The DSC and TGA thermograms can be found in Figure of the Supporting Information.

Finally, the printing by LDM of the epoxy vitrimer containing 37 wt% of cellulose powder was attempted (see video). After 3D printing, objects were thermally cured following the same thermal process applied for the neat vitrimer and its composite, i.e., heating at 200 °C for 6 h.

As it can be observed in Fig. 15 (top), the composite with 37 wt% of cellulose powder was successfully printed both in the form of a 20 × 20 mm^2 cube and in the form of a cylinder of 20 mm height and diameter of 20 mm. These results confirm that the composite vitrimer has the rheological properties required for LDM, i.e., the vitrimer is suitable for an extrusion-based 3D printing once the rheology is tailored with the aid of a filler.

After the curing cycle, the shape of the composite pieces was almost retained as it is shown in Fig. 15 (bottom): at the bottom of the objects a certain deformation is detectable, more evident for the cube. Also, some defects are present at the external surface due to the release of acetic acid from the catalyst and/or moisture from the cellulose powder.
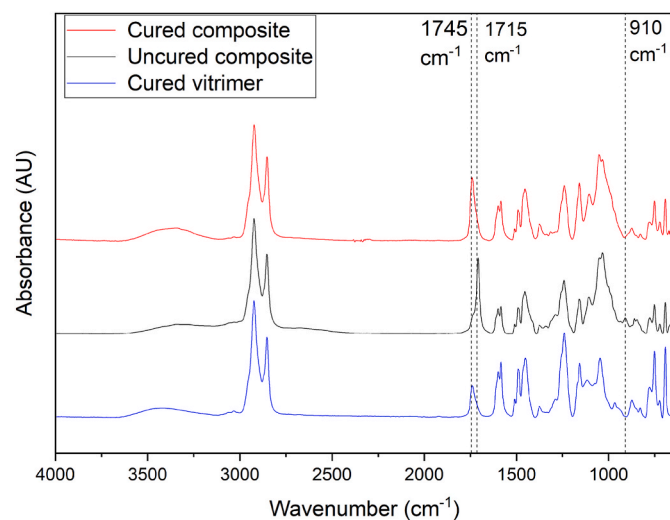
Fig. 14. ATR-FT-IR spectra of the uncured and cured composite with 37 wt% of cellulose filler, compared to the spectra of the cured vitrimer.

Table 3
T_g values by DSC, and TGA thermal degradation temperatures and residual mass at different temperature for cured vitrimer, cured composite and cured recycled composite samples.

Material	T_g (°C)	T_5 (°C)	T_{50} (°C)	$m_{800°C}$ (%) Under N$_2$
Cured vitrimer	−13	319	443	6
Cured composite	−15	290	423	13
Cured recycled composite	−21	297	414	9

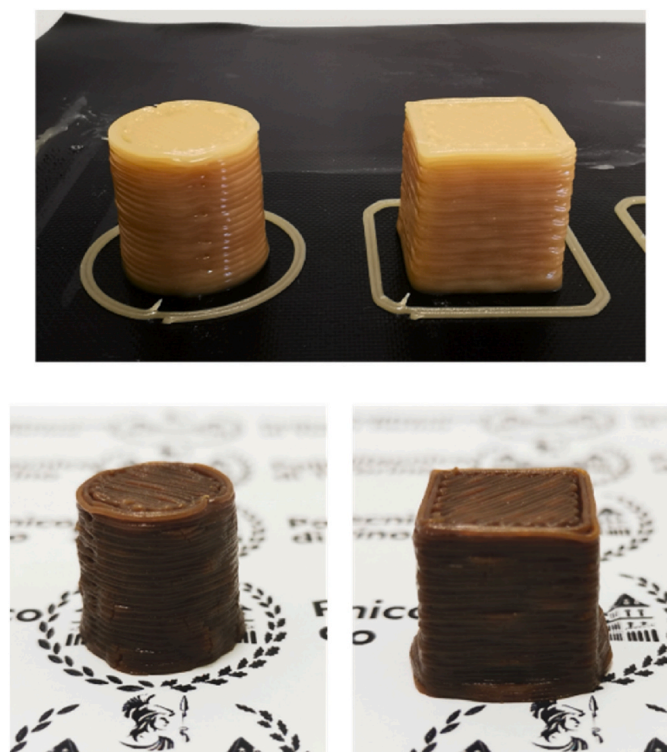**Fig. 15.** Picture of printed parts before (top) and after curing (bottom), made with the composite epoxy vitrimer with 37 wt% of cellulose filler.

Overall, it is proved that the fully biobased vitrimer composite designed in this work is recyclable and printable by LDM. Although the printing tests are preliminary, these results are interesting as they are in line with the current research trends for sustainability and with the perspectives of research in additive manufacturing. In fact, it was recently pointed out that too few vitrimers are available for 3D printing [H. [43]], among which the biobased ones are rare. Moreover, in the specific field of LDM no example regarding vitrimers is reported yet. As mentioned in the introduction, with respect to other AM technologies suitable for vitrimers, i.e. stereolithography (SLA), digit light processing (DLP) and fused deposition modeling (FDM), LDM is competitive as it works at room temperature, needs a simple set up, and has good capabilities for producing large size pieces. Therefore, coupling a sustainable technology and a sustainable material is very promising.

Benchmarking further the obtained hybrid network against similar epoxy vitrimers, our polyester-cellulose system requires similar temperatures and longer processing time for being reprocessed. At the same time, it has a relevant advantage versus its homologues: thanks to its viscoelastic properties it requires neither a precrosslinking step (precuring) before printing nor heating during extrusion [[20]].

4. Conclusions

In this work, we proposed for the first time the processing of a fully biobased epoxy vitrimer composite by Liquid Deposition Modelling (LDM) and proved the suitability of this simple AM technology for processing recyclable epoxy composites. The biobased sources of both the network precursors (i.e. the epoxide and the acid hardener) and the filler, the reversibility of the curing process and the sustainability of the processing technology, guarantee a much lower environmental impact compared to the fossil-based epoxides treated with traditional processing.

First, we successfully produced and characterized a new Covalent Adaptable Network based on a transesterification mechanism, made of up to 98% biobased compounds, i.e., a multifunctional epoxy resin

derived from cardanol and a hardener with a 100% biobased content. The developed material had a T_g below room temperature (thus it is rubbery), a topology freezing temperature around 71 °C but a quite high relaxation time, i.e., 20 min at 200 °C. The biobased vitrimer was successfully recycled and reprocessed thanks to a chemical recycling path, using ethylene glycol as a solvent. The recycled material maintained similar properties of the pristine vitrimer, with identical T_g ($T_g \approx -13$ °C) and unchanged thermal resistance as well as the viscoelastic properties.

The rheological behaviour of the vitrimer was not found suitable for LDM 3D printing and cellulose powder, a low-cost biobased filler, was added as a rheology modifier. Through a careful design of the viscoelastic properties, a formulation at relatively high cellulose content (37 wt%) was successfully printed without any pre-curing step and heating during extrusion. After modelling, the curing assured the retention of the shape of the printed pieces. The same process for recycling could be adopted for reprocessing the composite, allowing the recovery of the polymeric matrix and of the cellulose if needed.

CRediT authorship contribution statement

Jérôme M. Capannelli: Conceptualization, methodology, data curation, Writing – Original draft. Sara Dalle Vacche: Conceptualization, writing – review & editing. Alessandra Vitale: Writing – review & editing. Davide Beneventi: Funding acquisition, supervision. Khaoula Bouzidi: Methodology, writing – review & editing. Roberta Bongiovanni: Funding acquisition, project administration, supervision, conceptualization, writing – review & editing.

Declaration of competing interest

The authors declare that they have no known competing financial interests or personal relationships that could have appeared to influence the work reported in this paper.

Data availability

Data will be made available on request.

Appendix A. Supplementary data

Supplementary data to this article can be found online at https://doi.org/10.1016/j.polymertesting.2023.108172.

References

[1] J. Zheng, Z.M. Png, S.H. Ng, G.X. Tham, E. Ye, S.S. Goh, X.J. Loh, Z. Li, Vitrimers: current research trends and their emerging applications, Mater. Today 51 (2021) 586–625, https://doi.org/10.1016/j.mattod.2021.07.003.

[2] C.J. Kloxin, T.F. Scott, B.J. Adzima, C.N. Bowman, Covalent adaptable networks (CANs): a unique paradigm in cross-linked polymers, Macromolecules 43 (6) (2010) 2643–2653, https://doi.org/10.1021/ma902596s.

[3] Ze Ping Zhang, Min Zhi Rong, Ming Qiu Zhang, Polymer engineering based on reversible covalent chemistry: a promising innovative pathway towards new materials and new functionalities, Prog. Polym. Sci. 80 (2018) 39–93, https://doi.org/10.1016/j.progpolymsci.2018.03.002.

[4] J.M. Winne, L. Leibler, F.E. Du Prez, Dynamic covalent chemistry in polymer networks: a mechanistic perspective, Polym. Chem. 10 (45) (2019) 6091–6108, https://doi.org/10.1039/C9PY01260E.

[5] M. Podgórski, B.D. Fairbanks, B.E. Kirkpatrick, M. McBride, A. Martinez, A. Dobson, N.J. Bongiardina, C.N. Bowman, Toward stimuli-responsive dynamic thermosets through continuous development and improvements in covalent adaptable networks (CANs), Adv. Mater. 32 (20) (2020), 1906876, https://doi.org/10.1002/adma.201906876.

[6] D. Montarnal, M. Capelot, F. Tournilhac, L. Leibler, Silica-Like malleable materials from permanent organic networks, Science 334 (6058) (2011) 965, https://doi.org/10.1126/science.1212648.

[7] S. Guggari, F. Magliozzi, S. Malburet, A. Graillot, M. Destarac, M. Guerre, Vanillin-based epoxy vitrimers: looking at the cystamine hardener from a different perspective, ACS Sustain. Chem. Eng. 11 (15) (2023) 6021–6031, https://doi.org/10.1021/acssuschemeng.3c00379.

[8] I. Azcune, O. Ibon, Aromatic disulfide crosslinks in polymer systems: self-healing, reprocessability, recyclability and more, Eur. Polym. J. 84 (2016) 147–160, https://doi.org/10.1016/j.eurpolymj.2016.09.023.

[9] M. Chen, L. Zhou, Y. Wu, X. Zhao, Y. Zhang, Rapid stress relaxation and moderate temperature of malleability enabled by the synergy of disulfide metathesis and carboxylate transesterification in epoxy vitrimers, ACS Macro Lett. 8 (3) (2019) 255–260, https://doi.org/10.1021/acsmacrolett.9b00015.

[10] S. Dhers, G. Vantomme, L. Avérous, A fully bio-based polyimine vitrimer derived from fructose, Green Chem. 21 (7) (2019) 1596–1601, https://doi.org/10.1039/C9GC00540D.

[11] P. Taynton, K. Yu, R.K. Shoemaker, Y. Jin, H.J. Qi, W. Zhang, Heat- or water-driven malleability in a highly recyclable covalent network polymer, Adv. Mater. 26 (23) (2014) 3938–3942, https://doi.org/10.1002/adma.201400317.

[12] S.K. Schoustra, J.A. Dijksman, H. Zuilhof, M.M.J. Smulders, Molecular control over vitrimer-like mechanics – tuneable dynamic motifs based on the hammett equation in polyimine materials, Chem. Sci. 12 (1) (2021) 293–302, https://doi.org/10.1039/D0SC05458E.

[13] W. Denissen, G. Rivero, R. Nicolaÿ, L. Leibler, J.M. Winne, F.E. Du Prez, Vinylogous urethane vitrimers, Adv. Funct. Mater. 25 (16) (2015) 2451–2457, https://doi.org/10.1002/adfm.201404553.

[14] O.R. Cromwel, J. Chung, Z. Guan, Malleable and self-healing covalent polymer networks through tunable dynamic boronic ester bonds, J. Am. Chem. Soc. 137 (20) (2015) 6492–6495, https://doi.org/10.1021/jacs.5b03551.

[15] W.A. Ogden, Z. Guan, Recyclable, strong, and highly malleable thermosets based on boroxine networks, J. Am. Chem. Soc. 140 (20) (2018) 6217–6220, https://doi.org/10.1021/jacs.8b03257.

[16] W. Denissen, I. De Baere, W. Van Paepegem, L. Leibler, J.M. Winne, F.E. Du Prez, Vinylogous urea vitrimers and their application in fiber reinforced composites, Macromolecules 51 (5) (2018) 2054–2064, https://doi.org/10.1021/acs.macromol.7b02407.

[17] D. Zhang, H. Chen, Q. Dai, C. Xiang, Y. Li, X. Xiong, Y. Zhou, J. Zhang, Stimuli-mild, robust, commercializable polyurethane-urea vitrimer elastomer via N,N'-Diaryl urea crosslinking, Macromol. Chem. Phys. 221 (15) (2020), 1900564, https://doi.org/10.1002/macp.201900564.

[18] M. Capelot, M.M. Unterlass, F. Tournilhac, L. Leibler, Catalytic control of the vitrimer glass transition, ACS Macro Lett. 1 (7) (2012) 789–792, https://doi.org/10.1021/mz300239f.

[19] H. Fang, W. Ye, K. Yang, K. Song, H. Wei, Y. Ding, Vitrimer chemistry enables epoxy nanocomposites with mechanical robustness and integrated conductive segregated structure for high performance electromagnetic interference shielding, Compos. B Eng. 215 (2021) 108782, https://doi.org/10.1016/j.compositesb.2021.108782.

[20] Q. Shi, K. Yu, X. Kuang, X. Mu, C.K. Dunn, M.L. Dunn, T. Wang, H.J. Qi, Recyclable 3D printing of vitrimer epoxy, Mater. Horiz. 3 (1) (2017) 598–607, https://doi.org/10.1039/C7MH00043J.

[21] Q. Shi, K. Yu, M.L. Dunn, T. Wang, H.J. Qi, Solvent assisted pressure-free surface welding and reprocessing of malleable epoxy polymers, Macromolecules 49 (15) (2016) 5527–5537, https://doi.org/10.1021/acs.macromol.6b00858.

[22] X. Kuang, Y. Zhou, Q. Shi, T. Wang, H.J. Qi, Recycling of epoxy thermoset and composites via good solvent assisted and small molecules participated exchange reactions, ACS Sustain. Chem. Eng. 6 (7) (2018) 9189-97, https://doi.org/10.1021/acssuschemeng.8b01538.

[23] M. Peerzada, S. Abbasi, K.T. Lau, N. Hameed, Additive manufacturing of epoxy resins: materials, methods, and latest trends, Ind. Eng. Chem. Res 59 (14) (2020) 6375–6390, https://doi.org/10.1021/acs.iecr.9b06870.

[24] A.D. Valino, J.R.C. Dizon, A.H. Espera, Q. Chen, J. Messman, R.C. Advincula, Advances in 3D printing of thermoplastic polymer composites and nanocomposites, Prog. Polym. Sci. 98 (2019) 101162, https://doi.org/10.1016/j.progpolymsci.2019.101162.

[25] X. Zhao, P. Tian, Y. Li, J. Zeng, Biobased covalent adaptable networks: towards better sustainability of thermosets, Green Chem. 24 (11) (2022) 4363–4387, https://doi.org/10.1039/D2GC01325H.

[26] T. Vidil, A. Llevot, Fully biobased vitrimers: future direction toward sustainable cross-linked polymers, Macromol. Chem. Phys. 223 (13) (2022), 2100494, https://doi.org/10.1002/macp.202100494.

[27] M.A. Lucherelli, A. Duval, L. Avérous, Biobased vitrimers: towards sustainable and adaptable performing polymer materials, Prog. Polym. Sci. 127 (avril) (2022), 101515, https://doi.org/10.1016/j.progpolymsci.2022.101515.

[28] Y. Zhang, F. Ma, L. Shi, Bin Lyu, et al., Recyclable, repairable and malleable bio-based epoxy vitrimers: overview and future prospects, Curr. Opin. Green Sustainable Chem. 39 (février) (2023), 100726, https://doi.org/10.1016/j.cogsc.2022.100726.

[29] K.L. Chong, J.C. Lai, R.A. Rahman, N. Adrus, Z.H. Al-Saffar, A. Hassan, T.H. Lim, M.U. Wahit, A review on recent approaches to sustainable bio-based epoxy vitrimer from epoxidized vegetable oils, Ind. Crop. Prod. 189 (2022) 115857, https://doi.org/10.1016/j.indcrop.2022.115857.

[30] F. Jaillet, E. Darronan, A. Ratsimihety, R. Auvergne, B. Boutevin, S. Caillol, New biobased epoxy materials from cardanol: new biobased epoxy materials from cardanol, Eur. J. Lipid Sci. Technol. 116 (1) (2014) 63–73, https://doi.org/10.1002/ejlt.201300193.

[31] K. Bouzidi, D. Chaussy, A. Gandini, R. Bongiovanni, D. Beneventi, 3D printable fully biomass-based composite using poly(furfuryl alcohol) as binder and cellulose as a filler, Carbohydr. Polym. 293 (2022), 119716, https://doi.org/10.1016/j.carbpol.2022.119716.

[32] A. Demongeot, S.J. Mougnier, S. Okada, C. Soulié-Ziakovic, F. Tournilhac, Coordination and catalysis of Zn 2+ in epoxy-based vitrimers, Polym. Chem. 7 (27) (2016) 4486–4493, https://doi.org/10.1039/C6PY00752J.

[33] S. Dalle Vacche, A. Vitale, R. Bongiovanni, Photocuring of epoxidized cardanol for biobased composites with microfibrillated cellulose, Molecules 24 (21) (2019) 3858, https://doi.org/10.3390/molecules24213858.

[34] K. Kretzschmar, K.W. Hoffmann, Reaction enthalpies during the curing of epoxy resins with anhydrides, Thermochim. Acta 94 (1) (1985) 105–112, https://doi.org/10.1016/0040-6031(85)85250-3.

[35] K. Yu, P. Taynton, W. Zhang, M.L. Dunn, H.J. Qi, Influence of stoichiometry on the glass transition and bond exchange reactions in epoxy thermoset polymers, RSC Adv. 4 (89) (2014) 48682–48690, https://doi.org/10.1039/C4RA06543C.

[36] I. Taketo, M. Hayashi, Critical effects of branch numbers at the cross-link point on the relaxation behaviors of transesterification vitrimers', Macromolecules 55 (15) (2022) 6661–6670, https://doi.org/10.1021/acs.macromol.2c00560.

[37] M. Hayashi, Y. Ryoto, Fair investigation of cross-link density effects on the bond-exchange properties for trans-esterification-based vitrimers with identical concentrations of reactive groups, Macromolecules 53 (1) (2020) 182–189, https://doi.org/10.1021/acs.macromol.9b01896.

[38] M. Chen, H. Si, H. Zhang, L. Zhou, W. Yeping, L. Song, M. Kang, Xiu-Li Zhao, The crucial role in controlling the dynamic properties of polyester-based epoxy vitrimers: the density of exchangeable ester bonds, Macromolecules 54 (21) (2021) 10110–10117, https://doi.org/10.1021/acs.macromol.1c01289.

[39] Leslie Howard Sperling, Introduction to Physical Polymer Science, fourth ed., J. Wiley & sons, New York, 2006.

[40] F.I. Altuna, C.E. Hoppe, J.J. Williams Roberto, Epoxy vitrimers with a covalently bonded tertiary amine as catalyst of the transesterification reaction, Eur. Polym. J. 113 (2019) 297–304, https://doi.org/10.1016/j.eurpolymj.2019.01.045.

[41] A. M'Barki, L. Bocquet, A. Stevenson, Linking rheology and printability for dense and strong ceramics by direct ink writing, Sci. Rep. 7 (1) (2017) 6017, https://doi.org/10.1038/s41598-017-06115-0.

[42] C. Thibaut, « Development of Fibrous Cellulosic Materials for the Production of Bio-Based 3D Printed Objects by Extrusion », PhD Thesis, University of Grenoble Alpes, 2020, p. 242.

[43] H. Zhang, J. Cui, G. Hu, B. Zhang, Recycling strategies for vitrimers, Int. J. Soc. Netw. Min. 13 (2022) 367–390, https://doi.org/10.1080/19475411.2022.2087785.